Influence of the Angle Subtended by the Positively Charged Helix Face on the Membrane Activity of Amphipathic, Antibacterial Peptides†

Torsten Wieprecht,*,‡,§ Margitta Dathe,‡ Richard M. Epand,§ Michael Beyermann,‡ Eberhard Krause,‡ W. Lee Maloy,|| Dorothy L. MacDonald,|| and Michael Bienert‡

Forschungsinstitut für Molekulare Pharmakologie, Alfred Kowalke Strasse 4, D-10315 Berlin, Germany, Department of Biochemistry, McMaster University, Health Science Centre, Hamilton, Ontario L8N 3Z5, Canada, and Magainin Pharmaceuticals, Inc., 5110 Campus Drive, Plymouth Meeting, Pennsylvania 19462

Received June 11, 1997; Revised Manuscript Received August 5, 1997⊗

ABSTRACT: To investigate the influence of the angle subtended by the positively charged helix face on membrane activity, six amphipathic α-helical peptides with angles between 80° and 180°, but with retained hydrophobicity, hydrophobic moment, and positive overall charge, were designed starting from the sequence of the antibacterial peptide magainin 2. CD investigations revealed that all analogs are in an α-helical conformation in vesicle suspension. The ability of the peptides to induce dye release from negatively charged phosphatidylglycerol (PG) vesicles decreased with increasing angle. However, peptides with a large angle of positively charged residues (140−180°) exhibited a considerably higher permeabilizing activity at zwitterionic phosphatidylcholine (PC) and mixed PC/PG (3:1) vesicles than analogs with a small angle (80−120°). In addition, analogs with large angles were more active in antibacterial and hemolytic assays. The antibacterial specificity of these analogs was decreased. Binding investigations showed that peptide binding is favored by a large angle and a high content of negatively charged phospholipid. In contrast, a small angle and a low negative membrane charge enhanced the membrane-permeabilizing efficiency of the bound peptide fraction. All analogs stabilized the bilayer phase of phosphatidylethanolamine over the inverted hexagonal phase. Therefore, a class L mechanism of permeabilization can be excluded. Furthermore, the analogs do not act by the induction of positive curvature strain or by a "carpet-like" mechanism. Our results are in accordance with a pore mechanism: The membrane-permeabilizing efficiency of analogs with enhanced angle of positively charged residues is reduced due to electrostatic repulsion between adjacent helices within the pore, thus resulting in a decreased pore-forming probability and/or pore destabilization.

Over the past decades numerous membrane-lytic peptides have been isolated from insects, amphibians, and mammals. Among them are melittin from bee venom (*1*), mastoparans from wasp venom (*2*, *3*), cecropins from insects (*4*, *5*), defensins from mammalian neutrophils (*6*), and magainins from frog skin (*7*).

Membrane-lytic peptides can broadly be classified into cytolytic peptides, which are active against prokaryotic as well as eukaryotic cells, and antimicrobial peptides with a specificity for prokaryotic cell membranes. The discovery of members of the second class (e.g. magainins, cecropins), resulted in an increasing effort to develop antimicrobial peptides as alternatives to conventional antibiotics (for review see ref 8).

By now it is well established that these peptides act by enhancing the permeability of membranes, thus perturbing their barrier function. In the first stage of the membrane-permeabilizing process the peptides bind to membranes by adopting an amphipathic, mostly α-helical secondary structure with the polar helix face exposed to the lipid headgroups and the hydrophobic face somewhat embedded into the lipid acyl chain region. In the subsequent stage, the peptides enhance the permeability of membranes either by forming pores through the membrane or by destabilizing the structure of the bilayer. Pore formation is connected with peptide−peptide association and perpendicular insertion into the bilayer (barrel-stave model, for review see ref 9) or with formation of peptide−lipid complexes with the peptide helixes oriented parallel to the bilayer normal and the lipid headgroups filling the spaces between the helixes (*10*, *11*). Bilayer destabilization can arise from the induction of either negative curvature strain increasing the tendency of the lipids to adopt inverted phases or positive curvature strain expanding the bilayer headgroup region and thus perturbing bilayer integrity (*12*−*14*). A "carpet-like" mechanism has been proposed for peptides which act at comparably high ratios of bound peptide per lipid (*15*, *16*).

Extensive studies have been performed to understand the relationship between structure and activity of antibacterial peptides (for reviews see refs 8, 17, and 18). An amphipathic, mostly α-helical conformation and a positive net charge have been recognized as major structural motifs which determine the membrane disturbing activity. Enhancement of the total cationic peptide charge often results in a higher antibacterial activity. This observation has been associated

† This work was supported in part by a scholarship of the German Academic Exchange Service (DAAD, T.W.) and by the Medical Research Council of Canada (MT-7654 to R.M.E.).

* To whom correspondence should be addressed (Forschungsinstitut für Molekulare Pharmakologie).

‡ Forschungsinstitut für Molekulare Pharmakologie.

§ McMaster University.

|| Magainin Pharmaceuticals.

⊗ Abstract published in *Advance ACS Abstracts,* October 1, 1997.

S0006-2960(97)01398-6 CCC: $14.00

with a higher binding affinity of such peptides to the negatively charged bacterial membrane. Recently, investigations of cationic, amphipathic model peptides (*19*) and paradaxin analogs (*20*) revealed that helicity is more important for hemolytic activity than for the antibacterial effect. Variations in helicity can therefore lead to a modulation of the antibacterial specificity.

Previous studies of amphipathic antimicrobial peptides have also demonstrated the important role of hydrophobic moment and hydrophobicity for antibacterial, and hemolytic activity (*8*, *21*−*24*). Generally, peptides with higher hydrophobicity and hydrophobic moment show an enhanced antibacterial and hemolytic activity. However, hydrophobic interactions are reported to play a more important role for the hemolytic effect than for the antibacterial activity (*19*, *23*). In our recent work, we have demonstrated that a few, conservative substitutions in the amino acid sequence of the antibacterial peptide magainin 2 amide, which changed the hydrophobicity slightly but retained the hydrophobic moment and other structural properties of the peptide, strongly modulated membrane activity and selectivity at model and biological membranes (*24*).

According to the classification of Segrest et al. (*25*), many of the membrane-permeabilizing, α-helical peptides belong to the class L (lytic) amphipathic peptides. Peptides in this group are characterized by a high mean residue hydrophobic moment and a narrow hydrophilic helix face containing Lys residues, whose long side chains can allow increased penetration of the peptide into the membrane. The inverted wedge shape of class L peptides and the resulting bilayer destabilizing effect have been suggested to be the main cause for the membrane-perturbing effect (*13*, *14*). Since the apex angle of the inverted wedge is mainly influenced by the angle circumscribed by the positively charged Lys and Arg residues in the helical conformation, this angle can be expected to be an additional modulator of membrane activity. However, the effect of the angle of positively charged residues on membrane-lytic activity has not yet been systematically investigated.

Despite the existence of numerous structure−function studies on antibacterial peptides, our present knowledge is far from being able to reliably predict the influence of amino acid substitutions on antibacterial activity and selectivity. One reason for the limited predictability is owed to the fact that amino acid substitutions in peptides generally result in variations of more than one of the structural parameters influencing peptide membrane interaction. It is therefore often difficult to assign the observed effect to a change in one particular molecular property.

In our laboratory we follow the approach of elucidating the influence of structural parameters on membrane activity and selectivity by investigating peptide sets with variations in one structural parameter while the other parameters are kept largely constant (*19*, *23*, *24*). In a recent study individual structural features were found to be strong modulators of antibacterial and hemolytic activity (*23*). Here we investigated the influence of the angle subtended by the positively charged helix face on the membrane activity and selectivity of amphipathic, antibacterial peptides. Starting from the amino acid sequence of an analog of the antibacterial frog peptide magainin 2 amide (F^{16} substituted by W^{16}, angle subtended by the positively charged helix face: 120°, designated as 120°M2a), analogs were synthesized with smaller (80°, 100°) or larger (140°, 160°, 180°) positively charged angles but retained overall charge, secondary structure propensity, hydrophobicity and hydrophobic moment. We studied the secondary structure of the analogs by circular dichroism (CD)[1] spectroscopy and the interaction of the peptides with model membranes of varying surface charge and intrinsic curvature strain. Furthermore, we explored differences in activity to determine if they are modulated by differences in the membrane affinity and/or by changes in the membrane-disturbing activity of the bound peptide fraction. The membrane modulating properties of the analogs have been compared with the antibacterial and hemolytic activity. The results are discussed with regard to possible mechanisms of action.

EXPERIMENTAL PROCEDURES

Materials. The lipids, 1-palmitoyl-2-oleoylphosphatidylcholine (POPC), 1-palmitoyl-2-oleoylphosphatidyl-DL-glycerol (POPG), dipalmitoleoylphosphatidylethanolamine (DPoPE) and *N*-methyl dioleoylphosphatidylethanolamine [(NMe)DOPE] were purchased from Avanti Polar Lipids, Inc. (Alabaster, AL). The Fmoc amino acids for peptide synthesis were obtained from Novabiochem (Bad Soden, Germany). All other chemicals were of analytical or reagent grade.

Peptide Synthesis. Peptides were synthesized by automated solid-phase methods using standard Fmoc chemistry on Tenta Gel S RAM resin (0.21 mmol/g; RAPP Polymere, Tübingen, Germany) in the continuous-flow mode on a MilliGen 9050 (Millipore, MA) peptide synthesizer (*26*). Purification was carried out by preparative high-performance liquid chromatography (HPLC) on PolyEncap A300, 10 μm (250 × 20 mm i.d.) (Bischoff Analysentechnik GmbH, Leonberg, Germany) to give final products >95% pure by HPLC analysis. All peptides were characterized by matrix-assisted laser desorption ionization mass spectrometry (MALDI II; Kratos, Manchester, U.K.) with peptide content of lyophilized samples being determined by quantitative amino acid analysis (LC 3000, Biotronik-Eppendorf, Germany).

Vesicle Preparation. A lipid film was dried overnight under high vacuum for all kinds of vesicles. Large unilamellar vesicles (LUVs) for dye releasing experiments were prepared by the extrusion technique (*27*) as follows: after the dried lipid in dye-buffer solution [for POPC, POPC/POPG (3:1), and POPG LUVs, 70 mM calcein, 10 mM Tris, 0.1 mM EDTA (pH 7.4); for (NMe)DOPE, 12.5 mM ANTS, 45 mM DPX, 10 mM Tris, 22.5 mM NaCl, 1 mM EDTA (pH 10.0)] was vortexed, the suspension was freeze−thawed in liquid nitrogen for six cycles and extruded through polycarbonate filters (six times through two stacked 0.4 μm pore size filters followed by ten times through two stacked 0.1 μm pore size filters). Untrapped dye was removed from the LUVs by gel filtration on a Sephadex G75 column [eluent for POPC, POPC/POPG (3:1), and POPG LUVs, buffer

[1] Abbreviations: CD, circular dichroism; POPC, 1-palmitoyl-2-oleoylphosphatidylcholine; POPG, 1-palmitoyl-2-oleoylphosphatidyl-DL-glycerol; DPoPE, dipalmitoleoylphosphatidylethanolamine; (NMe)DOPE, *N*-methyl dioleoylphosphatidylethanolamine; HPLC, high-performance liquid chromatography; LUVs, large unilamellar vesicles; Tris, tris(hydroxymethyl)aminomethane; EDTA, ethylenediaminetetraacetic acid; SUVs, small unilamellar vesicles; ANTS, 1-aminonaphthalene-3,6,8-trisulfonic acid; DPX, *N*,*N*′-p-xylenebispyridinium bromide; MLVs, multilamellar vesicles; PIPES, 1,4-piperazinediethanesulfonic acid; DSC, differential scanning calorimetry; MIC, minimum inhibitory concentration; M2a, magainin 2 amide.

containing 10 mM Tris, 154 mM NaCl, 0.1 mM EDTA (pH 7.4); for (NMe)DOPE LUVs, buffer containing 6.5 mM Tris, 100 mM NaCl, 0.5 mM EDTA, 20 mg/L NaN_3 (pH 10)]. Lipid concentration was determined by phosphorus analysis (*28*).

Small unilamellar vesicles (SUVs) for CD measurements were prepared by sonication (under nitrogen, in ice water) of a lipid suspension [between 20 and 40 mM lipid in 10 mM Tris, 154 mM NaF, 0.1 mM EDTA (pH 7.4)] for 25 min using a titanium tip ultrasonicator. Titanium debris was removed by centrifugation. Dynamic light scattering experiments confirmed the existence of a main population of vesicles (more than 95% mass content) with a mean diameter of 41 ± 1 nm (polydispersity index: 0.3).

Circular Dichroism Measurements. CD measurements of the peptide solutions were carried out on a Jasco 720 spectrometer between 200 and 260 nm in vesicle suspension at 23 °C. Minor contributions of circular dichroism and circular differential scattering of the SUVs were largely eliminated by subtracting the lipid spectra of the corresponding peptide-free suspensions. The helicity of the peptides was determined from the mean residue ellipticity [Θ] at 222 nm (*29*). All data are the mean of two independent measurements which do not deviate more than 5%.

Dye Release Assays. Aliquots of dye-containing vesicular suspensions (10−20 μL) were injected into a cuvette containing 2.5 mL of a stirred peptide solution [10 mM Tris, 154 mM NaCl, 0.1 mM EDTA (pH 7.4)]. Calcein release from vesicles was determined fluorometrically by measuring the decrease in self-quenching (excitation at 490 nm, emission at 520 nm) on a Perkin-Elmer LS 50B spectrofluorometer. The release of co-entrapped ANTS/DPX from LUVs was observed by measuring the intensity increase of ANTS fluorescence due to dilution of the quencher DPX into the medium on a SLM AB-2 spectrofluorometer (excitation 360 nm, emission 530 nm). The fluorescence intensity corresponding to 100% release was determined by addition of Triton X-100 (100 μL, 10% v/v in water).

Binding Isotherms. Fluorescence-derived binding isotherms were determined from the increase of the tryptophan fluorescence intensity (*I*) of peptide solutions (three different concentrations between 0.5×10^{-6} and 1×10^{-5} M) after mixing with different amounts of LUVs. The peptide-lipid mixtures were stirred for 5 min before measurement to establish the binding equilibrium. Fluorescence intensities were measured on a SLM AB-2 spectrofluorometer with excitations between 280 and 290 nm and emission wavelengths close to the fluorescence maximum of the lipid-bound peptides with highest possible differences in the intensities of the bound and free peptide. The background intensity of the vesicles, measured with peptide-free vesicle samples, was subtracted from the observed intensities. The inner filter effect caused by light scattering of the lipid was corrected by the method of Lakowicz (*30*). The binding isotherms were calculated as described by Schwarz et al. (*31*) employing the following relations:

$$\text{(a) } F = (I - I_0)/I_0$$

where F is the relative signal, I the measured intensity in presence of lipid, and I_0 the measured intensity in absence of lipid, and

$$\text{(b) } F = F_\infty(c_B/c_P) = F_\infty(c_L/c_P) \times r$$

where F_∞ is F of the completely bound peptide, c_L the lipid concentration, c_P the total peptide concentration, c_B the lipid-bound peptide concentration, and $r = c_B/c_L$. From these equations and the mass conservation equation, the binding isotherm can be evaluated even under assumption of the existence of different lipid-associated states and varying F_∞ (for a detailed description see ref 31).

Binding isotherms from calcein-releasing experiments were derived according to Matsuzaki et al. (*32*). Briefly, dose-response curves were determined by measuring peptide-induced dye release at three different lipid concentrations between 5 and 100 μM. Plotting the total peptide concentration, c_P, as a function of the lipid concentration, c_L, for a given releasing effect results in a linear correlation between these points. Employing the mass conservation equation $c_P = rc_L + c_F$, where c_F is the concentration of free peptide, values of r and c_F can be calculated for each of the linear correlations between c_P and c_L.

Binding of the peptides to DPoPE multilamellar vesicles (MLVs) was determined by a centrifugation assay. After the dried lipid was vortexed with different amounts of peptide [buffer: 20 mM PIPES, 154 mM NaCl, 1 mM EDTA, 20 mg/L NaN_3 (pH 7.4); lipid concentration 10 mg/mL], the suspension was incubated for 30 min at 37 °C followed by centrifugation at 12000*g* for 2 min. The peptide content in the supernatant (c_f) was determined fluorometrically (excitation at 280 nm, emission at 350−355 nm) by comparing the fluorescence intensities of the supernatants with a standard curve.

Differential Scanning Calorimetry. MLVs of DPoPE were made by vortex mixing the dried lipid in presence or absence of peptide in buffer [20 mM PIPES, 154 mM NaCl, 1 mM EDTA, 20 mg/L NaN_3 (pH 7.4); lipid concentration 10 mg/mL]. The vesicle suspension and the buffer for the reference cell were degassed under vacuum. The bilayer to hexagonal phase transition temperature of the lipid was measured using a MC-2 high-sensitivity differential scanning calorimeter (Microcal, Amherst, MA). The heating scan rate was 39 K/h. The phase transition was fitted to a single van't Hoff component and the transition temperature (T_H) was obtained from the fitted curve.

Hemolytic Assay. The hemolytic activity of the peptides was determined using human red blood cells as described previously (*19*). In brief, the suspensions containing the peptide and 1.8×10^8 cells/mL were incubated for 30 min at 37 °C. After cooling in ice water and centrifugation an aliquot of the supernatant was dissolved with 0.5% NH_4OH and the optical density was measured at 540 nm. Peptide concentrations causing 25% hemolysis (EC_{25}) were derived from the dose−response curves. Values determined in repeat experiments differed by less than 5%.

Antibacterial Studies. Antimicrobial susceptibility testing was performed using a modification of the National Committee for Clinical Laboratory Standards (NCCLS) microdilution broth assay (1993). Mueller Hinton broth (BBL, Cockeysville, MD) was used for diluting the peptide stock solution and for diluting the bacterial inoculum. The inoculum was prepared from midlogarithmic phase cultures. The final concentration of bacteria in the wells was between 1 and 5×10^5 CFUs/mL. The final concentration of peptide solution ranged from 0.25 to 256 μg/mL in 2-fold dilutions. Peptides were tested in duplicate. The microtiter plates were incubated overnight at 37 °C, and the absorbance was read at 630 nm. The minimum inhibitory concentration (MIC)

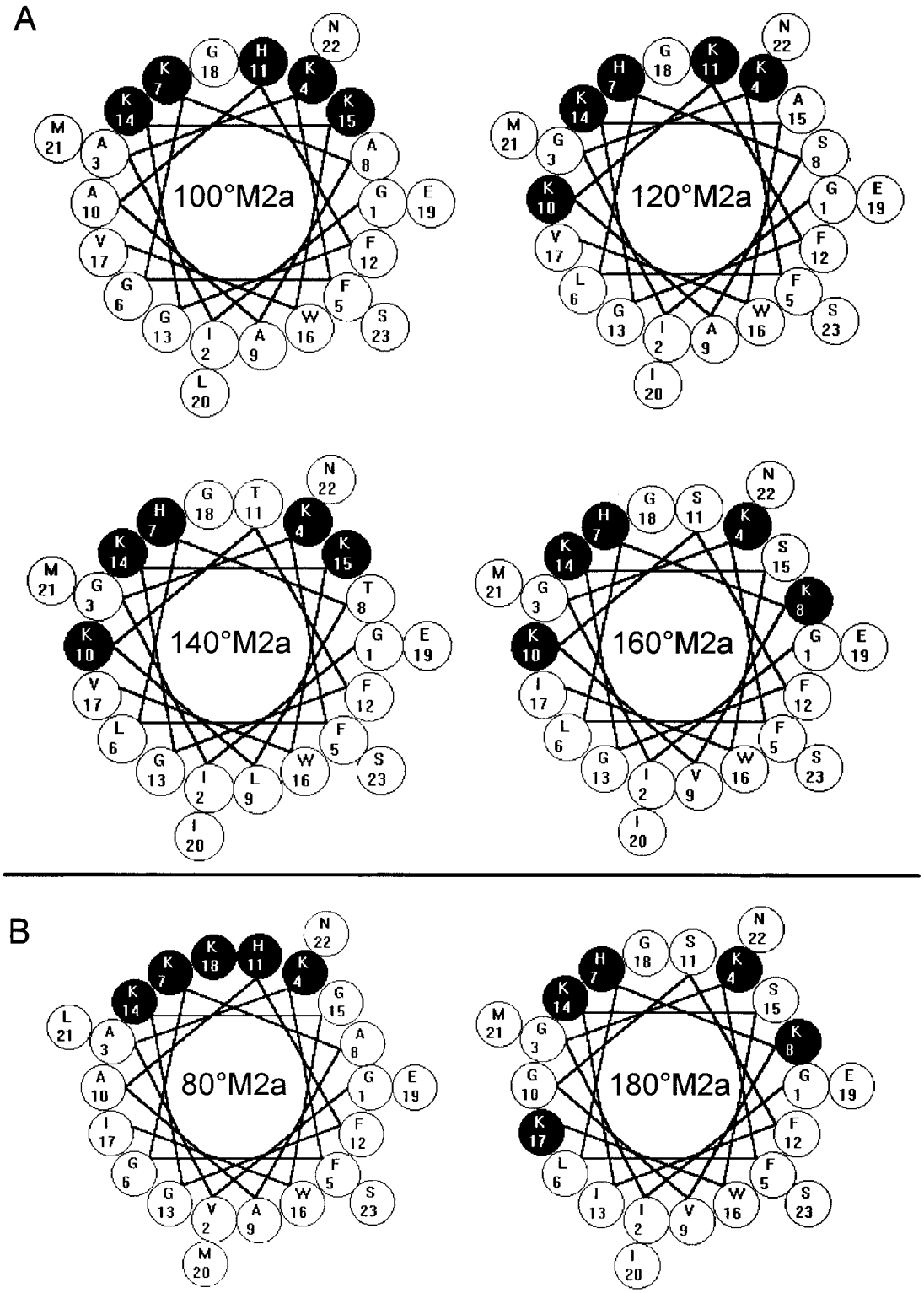

FIGURE 1: Helical wheel projection of peptides with variations in the positively charged angle. Black circles refer to residues with positively charged side chains, and white circles to all other residues. The charge of the His residue depends on the experimental conditions (p$K_a \approx$ 6.5: probably uncharged in solution at pH 7.4 but positively charged when bound to negatively charged vesicles).

is defined as the lowest concentration of peptide that completely inhibits growth.

RESULTS

Peptide Design. The positively charged residues (four lysine and one histidine) comprise an angle of 120° in the helical wheel projection of magainin 2 amide (M2a) as well as [Trp[16]]-magainin 2 amide (120°M2a) (Figure 1A). It was previously shown that substitution of Phe[16] in M2a by Trp minimally influenced bioactivity or activity on model membranes (*23*, *33*, *34*). Starting from 120°M2a, peptides with a higher or lower angle subtended by the positively charged helix face were synthesized considering the following rules: (i) The number and the type of the charged amino acids were maintained in all the analogs to avoid changes in the peptide overall charge and hence in the electrostatic interaction with negatively charged membrane components. (ii) Since hydrophobic moment and hydrophobicity have been shown to be strong modulators of membrane activity, the hydrophobicity and the hydrophobic moment based on

Table 1: Amino Acid Sequences, Angles Subtended by the Positively Charged Helix Face (Φ), Mean Residue Hydrophobicities (*H*), Hydrophobic Moments (μ), and Directions of the Hydrophobic Moment (*D*) of the Peptides[a]

peptide	amino acid sequence	Φ (deg)	*H*	μ	*D* (deg)
80°M2a	GVAKF GKAAA HFGKG WIKEM LNS (NH_2)	80	−0.045	0.281	−86
100°M2a	GIAKF GKAAA HFGKK WVGEL MNS (NH_2)	100	−0.045	0.288	−79
120°M2a	GIGKF LHSAK KFGKA WVGEI MNS (NH_2)	120	−0.046	0.277	−90
140°M2a	GIGKF LHTLK TFGKK WVGEI MNS (NH_2)	140	−0.049	0.288	−83
160°M2a	GIGKF LHKVK SFGKS WIGEI MNS (NH_2)	160	−0.047	0.288	−80
180°M2a	GIGKF LHKVG SFIKS WKGEI MNS (NH_2)	180	−0.047	0.281	−81

[a] The one-letter code for amino acids is used. Positively charged angles were estimated assuming an ideal α-helical conformation. Mean residue hydrophobicities and hydrophobic moments per residue were calculated using the Eisenberg consensus scale of hydrophobicity (*35*). The direction of the hydrophobic moment was calculated relative to Gly^1 in the helical wheel (see Figure 1).

the Eisenberg consensus scale (*35*) were kept constant for all analogs. (iii) The position of the Glu^{19} (negatively charged) and the Ser^{23} (located in the hydrophobic region) were retained to avoid changes in the effects caused by these residues which could superimpose effects of the positively charged angle.

The following procedure has been employed for peptide design: In the first step the angle of the positively charged helix face was reduced or increased by exchanging noncharged and charged amino acids at the positively charged/noncharged interface or within the positively charged region. For example, to enhance the angle from 120° to 180° Val^{17} of 120°M2a was exchanged for Lys^{10} and Ser^8 for Lys^{11}. Since enhancement or reduction of the angle circumscribed by the positively charged residues results in a lower or higher hydrophobic moment, respectively, further substitutions were necessary in a subsequent step to maintain the hydrophobic moment. To avoid changes of the overall peptide hydrophobicity during this procedure, the hydrophobic moment was corrected by simultaneous substitution of amino acids in the hydrophilic and hydrophobic helix face which restored the hydrophobic moment but did not affect the peptide overall hydrophobicity. In the case of the design of 180°M2a, after enhancement of the angle circumscribed by positively charged residues, subsequent substitutions of Ala^9 by Val, Val^{10} by Gly, Gly^{13} by Ile, and Ala^{15} by Ser were necessary to readjust the hydrophobic moment.

The sequences and helical wheel presentations of 120°M2a and the originally derived analogs 100°M2a, 140°M2a and 160°M2a are given in Table 1 and Figure 1A, respectively. Since initial investigations of the biological activity (*23*) and the activity at model membranes revealed a completely unexpected behavior of the peptides, two additional analogs (80°M2a and 180°M2a, Figure 1B) were synthesized and investigated to confirm the correlation between membrane activity and angle subtended by the positively charged helix face.

The biophysical properties of the peptides are summarized in Table 1. All peptides have a very similar mean residue hydrophobicity and hydrophobic moment of -0.047 ± 0.002 and 0.283 ± 0.006, respectively. The direction of the hydrophobic moment with respect to the position of Gly^1 in the helical wheel presentation ranges for all analogs between −79° and −90°. Since one amino acid occupies 20° in the helical wheel projection, the deviations in the direction of the hydrophobic moment are sufficiently low.

CD Investigations. All peptides adopt an unordered conformation in Tris-buffered saline (data not shown). The spectra of the peptides in the presence of POPG SUVs and POPC/POPG (3:1) SUVs are typical for α-helical conformations as reflected by the negative ellipticity at 207 and 222 nm (Figure 2). The helical content of the peptides was calculated to range between 75% and 91% (Table 2). Titration experiments of peptide solutions with vesicle suspensions revealed that all analogs are in a completely membrane-bound state at a lipid to peptide ratio of 166 [an exception is 80°M2a on POPC/POPG (3:1); data not shown]. At highly negatively charged POPG-vesicles the helicity values indicate that even at a lipid to peptide ratio as low as 17 more than 94% of the analogs are membrane-bound (Table 2).

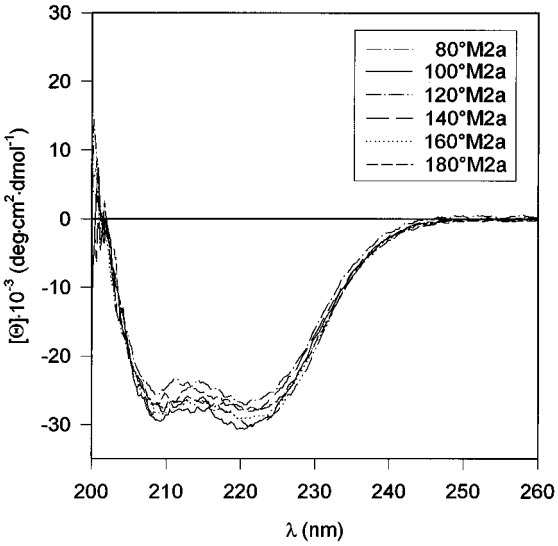

FIGURE 2: CD spectra of the analogs in presence of POPG SUVs at 23 °C. Peptide concentration was 50 μM in buffer (10 mM Tris, 154 mM NaF, 0.1 mM EDTA, pH 7.4), and the lipid to peptide ratio was 166.

Table 2: α-Helicity of the Peptides in SUV Suspensions[a]

lipid system: peptide	POPG SUVs (%) L/P = 17	POPG SUVs (%) L/P = 166	POPC/POPG (3:1) SUVs (%) L/P = 166
80°M2a	86	91	83
100°M2a	87	90	89
120°M2a	77	79	75
140°M2a	81	85	84
160°M2a	85	87	87
180°M2a	78	80	78

[a] Helical content was evaluated according to (*29*). The peptide concentration was 50 mM in buffer [10 mM Tris, 154 mM NaF, 0.1 mM EDTA (pH 7.4)]. All data are the mean of two independent measurements which do not deviate more than 5%.

Permeabilization of POPC, POPC/POPG (3:1), and POPC LUVs. The membrane-permeabilizing abilities of the peptides were investigated at highly negatively charged POPG LUVs, at moderately negatively charged POPC/POPG (3:1) LUVs, and at electrically neutral POPC LUVs employing a calcein releasing assay. The EC_{50} values of initial dye

Table 3: EC_{50} Values of Initial Rate of Calcein Release of the Peptides from LUVs of Different Surface Charge Density[a]

	EC_{50} (μM)		
peptide	POPG LUVs	POPC/POPG (3:1) LUVs	POPC LUVs
80°M2a	0.11 ± 0.01	3.80 ± 0.16	13.4 ± 1.5
100°M2a	0.21 ± 0.02	3.60 ± 0.20	20.5 ± 2.5
120°M2a	0.22 ± 0.02	2.40 ± 0.30	14.0 ± 2.0
140°M2a	0.42 ± 0.07	0.50 ± 0.05	0.39 ± 0.07
160°M2a	0.54 ± 0.01	0.90 ± 0.05	1.75 ± 0.25
180°M2a	0.75 ± 0.03	0.85 ± 0.06	0.43 ± 0.01

[a] EC_{50} values are the peptide concentrations inducing 50% dye release after 1 min at 23 °C. Values are the mean of two independent measures ± error of the mean. The lipid concentration was 25 mM in buffer [10 mM Tris, 154 mM NaCl, 0.1 mM EDTA (pH 7.4)].

release (50% dye release after 1 min), derived from the dose−response curves, were used as a measure of the membrane-disturbing effect (Table 3). All analogs permeabilize highly negatively charged POPG LUVs very effectively in a submicromolar concentration range. However, the activity decreases slightly with increasing positively charged angle.

A pronounced differentiation in the membrane-permeabilizing activity was found with zwitterionic POPC vesicles. The activity of the peptides follows the order 140°M2a ≈ 180°M2a > 160°M2a ≫ 120°M2a ≈ 80°M2a > 100°M2a (Table 3). Obviously, there is a separation of the analogs into two classes: Peptides with a high angle of positively charged residues (140°M2a, 160°M2a, 180°M2a) are much more active than peptides with a small angle (80°M2a, 100°M2a, 120°M2a). The same division has been observed at mixed POPC/POPG (3:1) LUVs. However, the differences between the group of more active peptides with a large angle and the less active peptides with small angles are less pronounced with mixed lipid vesicles.

Regarding the selectivity for negatively charged membranes, it is interesting to note that analogs with a low angle subtended by the positively charged helix face (80°M2a, 100°M2a, 120°M2a) are highly selective for negatively charged membranes (between 64- and 122-fold more active in permeabilizing POPG LUVs than POPC LUVs) whereas analogs with a high angle (140°M2a, 160°M2a, 180°M2a) are poorly or not at all selective.

Membrane-Binding and -Disturbing Activity at POPC/POPG (3:1) LUVs. The separation of the peptides on POPC-rich vesicles [POPC, POPC/POPG (3:1)] into two classes with different permeabilizing activity can be caused by differences in the lipid affinity of the peptides and/or by differences in the ability of the membrane-bound peptide fraction to disturb the bilayer structure. Binding isotherms of the peptides on POPC/POPG (3:1) LUVs were derived fluorometrically by titration of peptide solutions with vesicle suspensions (Figure 3). The binding affinity of the peptides to POPC/POPG (3:1) LUVs decreases in the order 140°M2a > 180°M2a > 160°M2a > 120°M2a > 100°M2a > 80°M2a. Hence, the order of the binding affinity correlates with the order of membrane-permeabilizing activity at POPC/POPG (3:1) LUVs (Table 3). The analog with the highest lipid affinity (140°M2a) has an about 92-fold higher apparent initial binding constant (K_{app}) than the peptide with the least affinity (80°M2a, Table 4).

The binding isotherms were correlated with the dye releasing experiments from POPC/POPG (3:1) LUVs (Figure 4A) in order to calculate the ratios of bound peptide per lipid

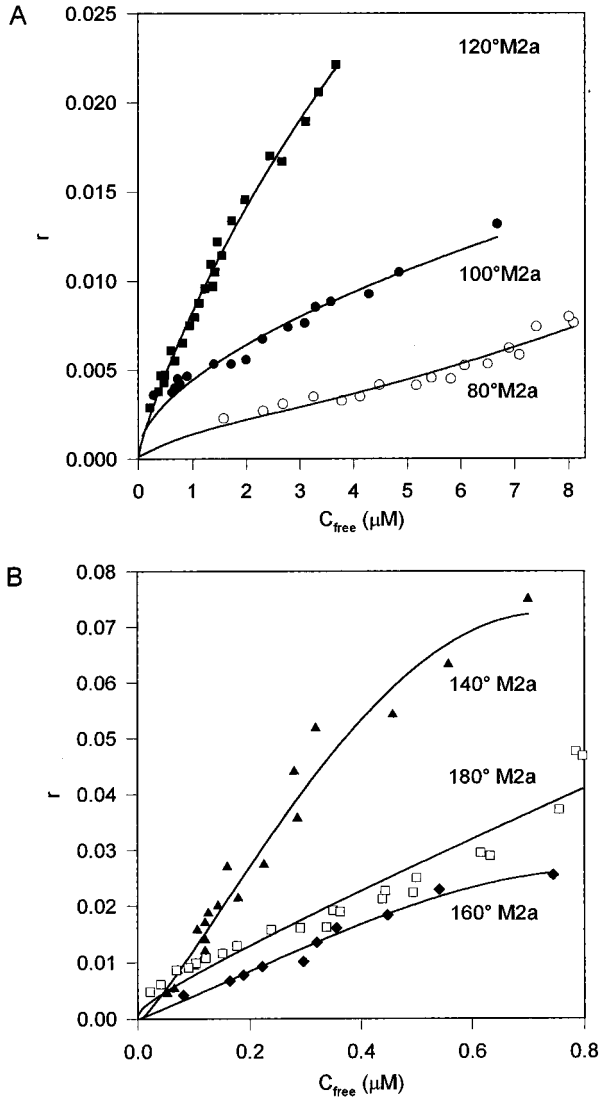

FIGURE 3: Binding isotherms of peptides with different positively charged angle on POPC/POPG (3:1) LUVs: (A) ○, 80°M2a; ●, 100°M2a; ■, 120°M2a, (B) ▲, 140°M2a; ◆, 160°M2a; □, 180°M2a. Isotherms were derived fluorometrically as described in Experimental Procedures.

Table 4: Characterization of Binding to and Permeabilization of POPC/POPG (3:1) LUVs: Apparent Binding Constants (K_{app}),[a] Ratio Bound Peptide per Lipid at Half-Maximal Dye Release ($r_{50\%}$), and Fraction of Bound Peptide at EC_{50} (F)[b]

peptide	K_{app} (M^{-1})	$r_{50\%}$	F (%)
80°M2a	1200	0.004	2.6
100°M2a	6400	0.008	5.6
120°M2a	10200	0.013	13.5
140°M2a	111000	0.014	70.0
160°M2a	42000	0.017	47.2
180°M2a	93000	0.020	58.8

[a] Apparent binding constants on POPC/POPG (3:1) LUVs were calculated from the initial slope of the binding isotherms (Figure 3). [b] Binding isotherms have been correlated with calcein-releasing experiments from POPC/POPG (3:1) LUVs (see Figure 4A).

corresponding to a given initial rate of calcein release (Table 4, Figure 4B). The ratio of bound peptide per lipid which induces 50% calcein release after one minute ($r_{50\%}$) was found to increase with increasing angle of positively charged residues. Whereas only four 80°M2a molecules per 1000 lipid molecules are necessary to induce 50% dye release, about 20 peptide molecules of 180°M2a per 1000 lipid molecules are required for the same effect. The order of

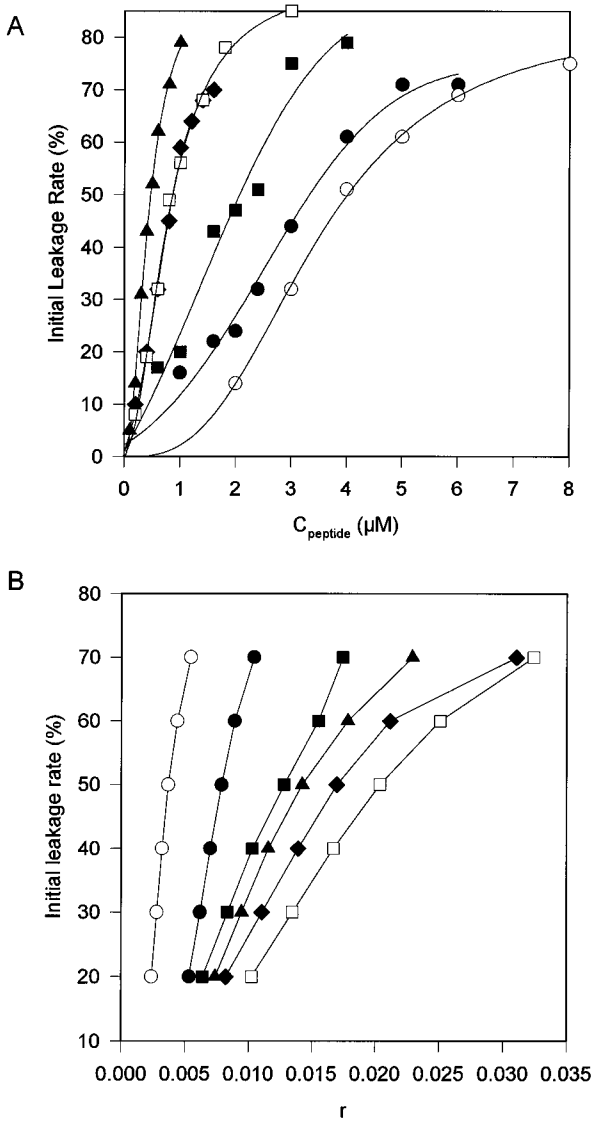

FIGURE 4: (A) Dependence of calcein leakage from POPC/POPG (3:1) LUVs on total peptide concentration. Calcein leakage is defined as the percent leakage after 1 min at a lipid concentration of 25 μM. (B) Relationship between the percent calcein leakage and the molar ratio of bound peptide per lipid (r). Symbols: ○, 80°M2a; ●, 100°M2a; ■, 120°M2a; ▲, 140°M2a; ◆, 160°M2a; □, 180°M2a.

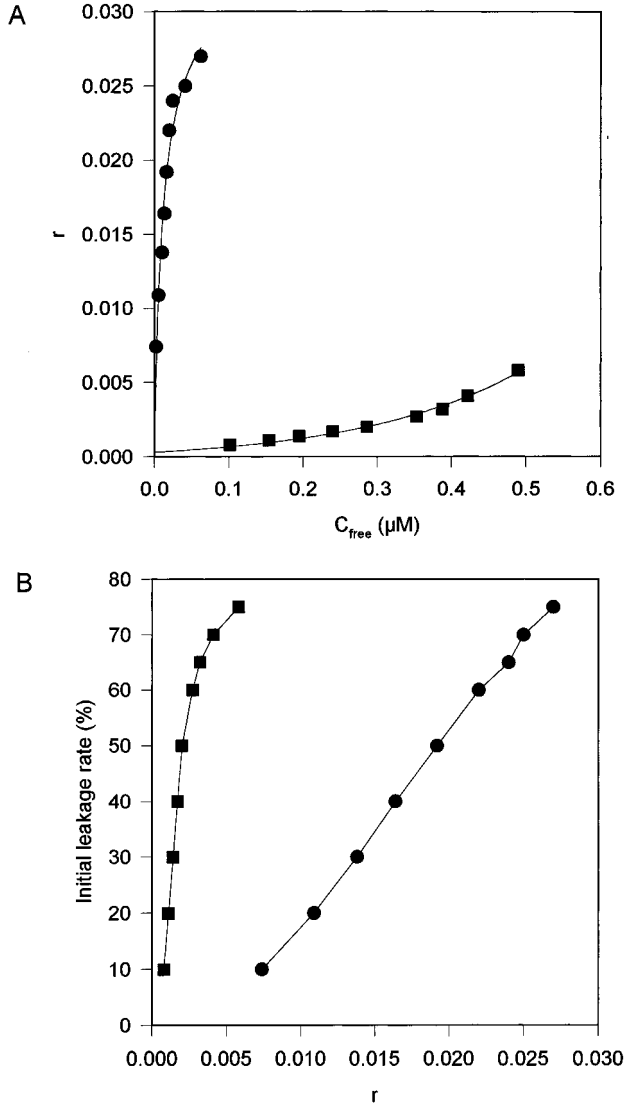

FIGURE 5: (A) Binding isotherms and (B) relationship between calcein leakage after 1 min and the molar ratio of bound peptide per lipid (r) of 140°M2a on POPG LUVs (●) and POPC LUVs (■). Binding was derived from calcein-releasing experiments as described in Experimental Procedures.

permeabilizing efficiency of the bound peptide fraction is roughly opposite to the order of the binding affinity. Analogs with a large angle of positively charged residues show a high binding affinity but a low membrane-permeabilizing efficiency of the bound peptide fraction, whereas peptides with a small angle are highly active when bound but possess a low binding affinity.

Influence of Vesicle Charge on Membrane-Binding and -Disturbing Activity of 140°M2a. Despite the positive peptide charge, and therefore an anticipated strong interaction with negatively charged lipids, 140°M2a and 180°M2a were found to be almost equally active in permeabilizing POPC and POPG LUVs (Table 3). To elucidate whether this behavior can be associated with an unusual high binding affinity to POPC vesicles or with an enhanced membrane-disturbing efficiency of the bound peptide fraction, binding isotherms of the 140°M2a analog were determined to POPC and POPG LUVs by studying the dependence of peptide-induced dye release on the lipid concentration (*32*). This method allows a direct derivation of the relation between initial rate of dye release and the ratio of bound peptide per lipid (r). The binding isotherms as well as the dependence of dye release on the ratio of bound peptide per lipid are given in Figure 5. 140°M2a shows a much higher binding affinity to negatively charged POPG LUVs ($K_{app} = 2 \times 10^6$ M^{-1}) than to zwitterionic POPC LUVs ($K_{app} = 7300$ M^{-1}). However, the membrane-permeabilizing efficiency of the bound peptide is considerably higher on POPC LUVs ($r_{50\%} = 0.002$) than on POPG LUVs ($r_{50\%} = 0.019$).[2] The dependence of binding and permeabilizing efficiency on membrane charge is confirmed by the investigations on POPC/POPG (3:1) LUVs ($K_{app} = 1.11 \times 10^5$ M^{-1}, $r_{50\%} = 0.014$; Table 4). Therefore, while the binding affinity of the peptide decreases with decreasing negative charge of the vesicles, the lytic efficiency of the bound peptide fraction increases.

Influence of Peptides on the $L_\alpha - H_{II}$ Phase Transition of DPoPE. Biological membranes contain large amounts of lipids which form inverted phases, if present in pure form, and induce intrinsic negative curvature strain as components

[2] It should be noted that a low $r_{50\%}$ value corresponds to a high efficiency of the bound peptide to permeabilize the membrane.

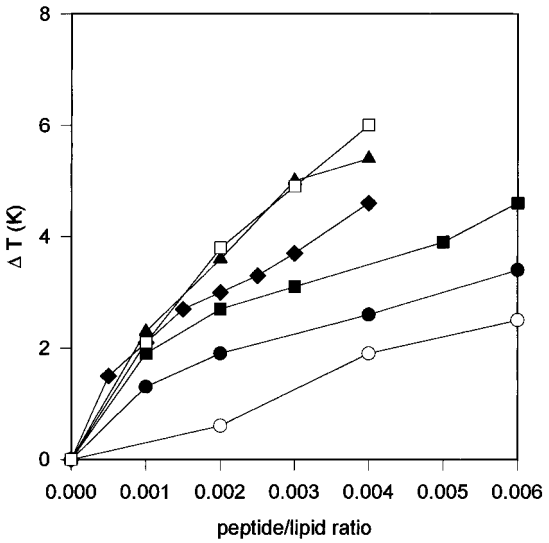

FIGURE 6: Dependence of the bilayer to hexagonal phase transition temperature (T_H) of DPoPE on the ratio of total peptide per lipid. The T_H of pure DPoPE was found to be 45.1 ± 0.4 °C (n = 7). Symbols: ○, 80°M2a; ●, 100°M2a; ■, 120°M2a; ▲, 140°M2a; ◆, 160°M2a; □, 180°M2a.

in biological and model membranes (e.g. phosphatidylethanolamine, cardiolipin-calcium, cholesterol, diacylglycerol). The shift in the bilayer to hexagonal ($L_\alpha-H_{II}$) phase transition temperature (ΔT_H) of DPoPE MLVs in the presence of a peptide is an indirect but sensitive measure, of whether the peptide is able to enhance or reduce negative curvature strain.

Figure 6 shows that all peptide analogs raised the bilayer to hexagonal phase transition temperature of DPoPE MLVs and hence stabilized the bilayer phase relative to the inverted hexagonal phase. The effectiveness of the peptides to stabilize the bilayer phase decreases in the order 180°M2a ≈ 140°M2a > 160°M2a > 120°M2a > 100°M2a > 80°M2a. However, it must be taken into consideration that the effect of peptides on the $L_\alpha-H_{II}$ phase transition depends on both, the membrane-binding affinity of the peptide as well as the effect of the bound peptide fraction. To evaluate the effectiveness of the bound peptide fraction to raise T_H, binding isotherms of the peptides to DPoPE MLVs were determined at 37 °C near the bilayer to hexagonal phase transition temperature employing a centrifugation assay (Figure 7A). Interestingly, the order of the binding affinities (140°M2a > 180°M2a > 160°M2a > 120°M2a > 100°M2a > 80°M2a) is essentially the same as the affinity order to POPC/POPG (3:1) LUVs. Calculation of the bound peptide fraction for each of the data points in Figure 6 allowed calculation of the dependence of ΔT_H on the bound peptide fraction (Figure 7B). The results show that the effectiveness of the bound peptide fraction to raise ΔT_H is similar for all of the peptides. The observed differences in the ability of the peptides to stabilize the bilayer phase over the hexagonal phase (Figure 6) are hence mainly dominated by differences in the membrane affinity of the peptides.

Dye Release from (NMe)DOPE LUVs. Dye-entrapped LUVs of (NMe)DOPE were used to study the effect of the peptides on model bilayers composed of a lipid with a tendency to form inverted phases. To elucidate the influence of the peptides on the membrane curvature strain we performed the experiments near the $L_\alpha-H_{II}$ phase transition temperature at 65° (T_H = 67 °C). Under these conditions

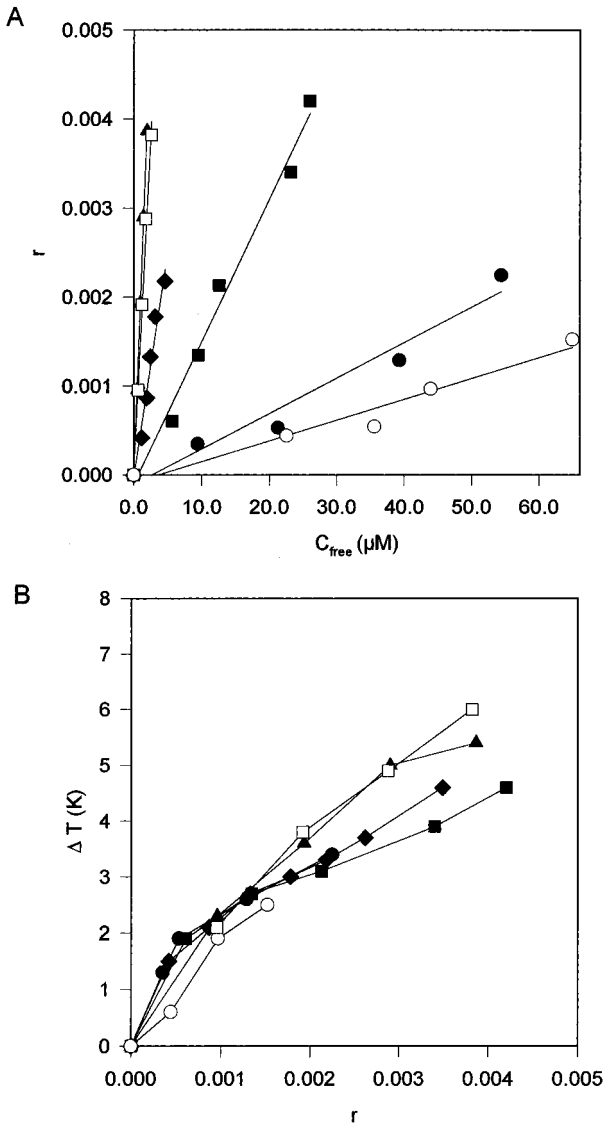

FIGURE 7: (A) Binding isotherms of peptides with different positively charged angle on DPoPE MLVs at 37 °C. Isotherms were derived by a centrifugation assay (see Experimental Procedures). Every data point is the mean of two independent measurements, which deviate not more than 8%. The apparent binding constants are 23 M^{-1} for 80°M2a, 40 M^{-1} for 100°M2a, 160 M^{-1} for 120°M2a, 2023 M^{-1} for 140°M2a, 509 M^{-1} for 160°M2a, and 1505 M^{-1} for 180°M2a. (B) Dependence of the bilayer to hexagonal phase transition temperature (T_H) of DPoPE on the ratio of bound peptide per lipid. Symbols: ○, 80°M2a; ●, 100°M2a; ■, 120°M2a; ▲, 140°M2a; ◆, 160°M2a; □, 180°M2a.

(NMe)DOPE LUVs showed a leakage of 45% ± 4% (n = 7) within the first 200 s in the absence of peptide. Analogs with a large angle of positively charged residues (140°, 160°, 180°M2a) showed a biphasic behavior (Figure 8.). They enhanced the leakage at low peptide concentrations but inhibited temperature-induced leakage at higher peptide concentrations. Analogs with a narrow angle (80−120°) increased the leakage at low concentrations. At higher concentrations the leakage increase stopped and remained almost constant up to 35 μM (for example see 120°M2a, Figure 8).

Biological Activity. The antibacterial activity of the peptides was tested against the Gram-negative bacteria *Escherichia coli* and *Pseudomonas aeruginosa* as well as against the Gram-positive bacteria *Staphylococcus aureus*. The hemolytic effect was determined as a measure of the toxicity against eukaryotic cells (Table 5). The minimum

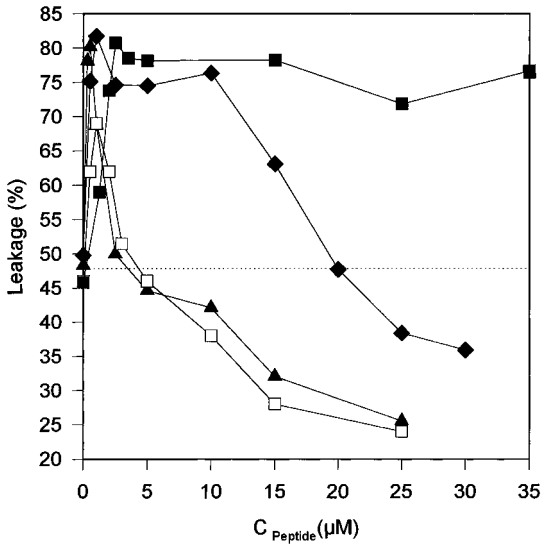

FIGURE 8: Dependence of dye leakage (ANTS/DPX) from (NMe)-DOPE LUVs on total peptide concentration at 65 °C. Dye release is defined as the percent leakage after 200 s at a lipid concentration of 25 μM. The temperature-induced dye release in absence of peptide was found to be 45% ± 4% ($n = 7$). Symbols: ■, 120°M2a; ▲, 140°M2a; ◆, 160°M2a; □, 180°M2a.

inhibitory concentrations against all three bacterial strains investigated was smaller for analogs with a large angle circumscribed by the positively charged residues (140−180°) than for peptides with small angles (80−120°). The separation of the analogs into two classes with different activities was even more pronounced for the hemolytic effect. Here, the EC_{25} values of hemolysis were found to range between 159 and 307 μM for the analogs with a narrow angle (80−120°) and between 15 and 24 μM for peptides with angles between 140 and 180°. Looking at the antibacterial specificity of the peptides it must be emphasized that the analogs with large angles are often less selective than analogs with small angles. So, the activity of the analogs with angles between 140 and 180° against *P. aeruginosa* is between 1- and 6-fold enhanced compared to 120°M2a, whereas the hemolytic effect is increased by factors between 11 and 18, thus reflecting a reduced antibacterial selectivity of these analogs compared to the 120°M2a peptide. Similarly, the activity of 140°M2a and 160°M2a against *E. coli* is 2−3-fold higher than for 120°M2a, but the hemolysis exhibits a larger increase of 13−18-fold. Thus, the [Trp^{16}]-analog of the native molecule is among the most selective for antibacterial activity.

DISCUSSION

The aim of this study was to investigate in detail the influence of the angle subtended by the positively charged amino acids on peptide-membrane interactions of amphipathic helical peptides. Starting from the amino acid sequence of the antibacterial peptide magainin 2 amide (M2a), we synthesized six peptides with angles circumscribed by the positively charged residues ranging between 80° and 180°. To avoid a superimposition of the effect of the angle subtended by the positively charged residues with effects of the overall charge, helical propensity, hydrophobicity and hydrophobic moment, these latter structural parameters were kept constant. CD investigations on the peptides bound to phospholipid vesicles revealed that all analogs exist in an α-helical conformation (Table 2). Lipid-bound M2a was recently found to be helical over the entire peptide chain (*33*, *36*). Since all peptides investigated show similar or even higher helicity values than measured for M2a (*33*), it is reasonable to conclude that the sequence modifications did not change the completely helical conformation of the peptide. This is a prerequisite for our investigations since significant secondary structure changes as a result of sequence modifications would lead to unpredictable changes in the expected positively charged angle and hydrophobic moment.

Dye release investigations from highly negatively charged POPG LUVs revealed a small, but significant reduction of the membrane-permeabilizing activity with increasing positively charged angle (Table 3). The dominance of electrostatic interactions between the peptide charges and the lipid headgroups is certainly responsible for the high membrane-permeabilizing activity and the weak differentiation among the analogs. For membranes with high phosphatidylcholine content [POPC/POPG (3:1), POPC] the relationship between angle and leakage is roughly opposite. Analogs with a small angle of positively charged residues (80−120°) are considerably less active than analogs with a large angle (140−180°). This separation into two differently active classes is especially pronounced with electrically neutral POPC LUVs, resulting in the conclusion that hydrophobic interactions are responsible for the different activities of the analogs. Likewise, peptides with a small angle (80−120°) are less active against bacteria and erythrocytes than analogs with larger angles (140−180°) (Table 5).

Interestingly, peptides with a larger angle show, compared to 120°M2a, a reduced selectivity for the permeabilization of negatively charged over zwitterionic model membranes and for the antibacterial over the hemolytic effect. This correlation between reduced selectivity for negatively charged model membranes and reduced antibacterial specificity can be explained by the absence of negatively charged phospholipids in the outer leaflet of the erythrocyte membrane and the presence of these lipids in the outer membrane of Gram-negative bacteria and in the cell membrane of Gram-positive bacteria. Hence, whereas electrically neutral POPC LUVs seem to be a simple but suitable model system to describe the interaction of the peptides with erythrocytes, negatively charged POPC/POPG (3:1) LUVs are better to model the antibacterial effects of the peptides. In contrast, the lack of any correlation between biological effects and permeabilization of highly negatively charged POPG membranes shows that these are not an appropriate model system for either cytoplasmic mammalian membranes or bacterial membranes.

Our finding that peptides with larger angle of positively charged residues are more active in permeabilizing biological and PC-rich model membranes than analogs with small angles is different from the observations of Tytler et al. (*13*). They investigated three peptides derived from a class L model peptide with positively charged angles of 100, 120, and 140°, respectively, and reported a decrease of the hemolytic activity with increasing angle. However, the analogs were designed by exchanging neighboring amino acids at the charged/uncharged interface without correction of the hydrophobic moment. Consequently, the peptides with smaller angles had an increased hydrophobic moment. Our recent biological investigation revealed that slight enhancement of the hydrophobic moment of amphipathic, antibacterial peptides, significantly enhanced hemolytic as well as antibacterial activity (*23*). Therefore, the enhanced hemolytic

Table 5: Antibacterial and Hemolytic Activity of the Peptides[a]

peptide	antibacterial activity MIC (μM) *E. coli* (ATCC 25922)	*P. aeruginosa* (ATCC 27853)	*S. aureus* (ATCC 29213)	hemolytic activity EC_{25} (μM)
80°M2a	>76	>76	>76	307
100°M2a	75	>75	>75	159
120°M2a	40	80	>80	271
140°M2a	13	13	13	15
160°M2a	19	19	76	20
180°M2a	5	36−73	73	24

[a] MIC is the minimum inhibitory concentration of bacterial growth. MIC values indicated as >75, >76, or >80 μM correspond to an antibacterial activity beyond the experimental range (>256 μg/mL). EC_{25} is the concentration inducing 25% of maximal lysis of human erythrocytes. EC_{25} is shown, since EC_{50} could not be determined for all analogs.

activity of peptides with smaller angles of positively charged residues described in the paper of Tytler et al. (*13*) may at least partially arise from the increased hydrophobic moment.

The binding investigations at POPC/POPG (3:1) LUVs showed that the order of peptide-binding correlates with the order of the peptides in membrane permeabilization (Figure 3, Table 3). Hence, a large angle (140−180°) favors the partitioning of the peptides into the lipid phase. Obviously, peptide partitioning does not only depend on peptide hydrophobicity but also on the relative size of the hydrophobic and the charged helical regions. Enhancement of the angle circumscribed by the positively charged residues, under the condition of an unchanged overall hydrophobicity and hydrophobic moment, results in a smaller hydrophobic domain with an increased hydrophobicity. It is reasonable to assume that incorporation of a smaller hydrophobic domain with an increased hydrophobicity is energetically favored. This conclusion is reinforced by the fact that the reversed phase HPLC retention times of the analogs with increased angle are also enhanced revealing a stronger interaction of these analogs with the hydrophobic stationary phase (data not shown).

However, a large angle is a disadvantage for the membrane-permeabilizing efficiency of the bound peptide: 20 molecules of 180°M2a have to be bound per 1000 lipid molecules to induce 50% dye release, whereas only 4 molecules of 80°M2a are necessary for the same effect. Comparing quantitatively the opposite influence of the angle subtended by the positively charged helix face on peptide-membrane binding (K_{app}) and membrane-disturbance [$r_{50\%}$, Table 4] with the overall membrane-permeabilizing effect (EC_{50} of dye release, Table 3), it can be concluded that binding overcompensates the permeabilizing efficiency of the bound peptide fraction and dominates the overall process of membrane permeabilization. A similar dominance of binding for the membrane-permeabilizing effect has recently been reported for a set of peptides with differences in the peptide hydrophobicity (*24*). However, the hydrophobicity-modified analogs showed a quite similar membrane-permeabilizing efficiency of the bound peptide fraction ($r_{50\%}$), whereas the analogs investigated in this study do not. This points to a considerable influence of the positively charged angle on the permeabilization step.

It is interesting to note that the ratios of bound peptide per lipid necessary to induce 50% dye release from POPC/POPG (3:1) LUVs ($r_{50\%}$, Table 4) follow the order of the EC_{50} values of dye release from POPG LUVs (Table 3). Binding studies of 140°M2a on POPG LUVs revealed a high binding affinity ($K_{app} = 2 \times 10^6$ M^{-1}) corresponding to a bound peptide fraction of more than 98% under the conditions of dye release ($C_{lipid} = 25$ μM). Moreover, at a lipid/peptide ratio as low as 17 more than 94% of all angle-modified analogs were bound to POPG vesicles as determined by CD spectroscopy (Table 2). It is therefore reasonable to assume that the dominance of electrostatic interactions and the unchanged overall charge within the peptide set result in comparable high degrees of binding during the dye release investigations. Consequently, the observed increase in the EC_{50} values of dye release from POPG LUVs with increasing angle of positively charged residues should reflect differences in the efficiency of the membrane-bound peptide fraction rather than differences in the degree of binding. Therefore, an opposite behavior in the macroscopic permeabilization effect on POPG and POPC/POPG (3:1) vesicles has its basis in the same microscopic principles. On both vesicle systems there is a decreasing permeabilization efficiency of the bound peptide fraction with increasing angle of positively charged residues. The strong, electrostatic-dominated accumulation on POPG LUVs prevents great differences in the fraction of peptide bound, and thus the order of the macroscopic effect corresponds to the order of the efficiency of the membrane-bound fraction. In contrast, the great differences in the peptide affinity for POPC/POPG (3:1) LUVs [see Table 4: fraction of bound peptide (F)] due to reduced electrostatic interactions overcompensate the effect of the permeabilizing efficiency for this vesicle system and result in an opposite observed effect.

Looking at the interplay of binding and permeabilization efficiency may also help to explain the apparently undifferentiated action of the positively charged 140°M2a on lipid systems with different negative surface charge. As expected, there is a strong increase in the binding affinity with increasing content of negatively charged phospholipid [K_{app}(POPC) = 7300 M^{-1}, K_{app}[POPC/POPG (3:1)] = 1.11 $\times 10^5$ M^{-1}, K_{app}(POPG) = 2.0 $\times 10^6$ M^{-1}]. However, the increased binding is compensated by a decreasing permeabilizing efficiency of the bound peptide fraction with increasing amount of negatively charged lipid [$r_{50\%}$(POPC) = 0.002, $r_{50\%}$[POPC/POPG (3:1)] = 0.014, $r_{50\%}$(POPG) = 0.019]. Apparently, strong electrostatic interactions between the peptide and lipid anchor the peptide in the headgroup region and hamper an effective membrane disturbance. The different effect of binding and permeabilizing efficiency has recently been described using an amphipathic model peptide (*19*). Comparable observations have also been reported for melittin (*37*) and mastoparan (*38*).

The binding isotherm of 140°M2a with POPC LUVs is characterized by an upward bending, characteristic of positive cooperativity. Positive cooperativity is often associated with a peptide−peptide association within the membrane. How-

ever, it may also arise from a structural change of the lipid bilayer due to peptide partitioning into the membrane. Therefore, further experiments would be necessary to elucidate the molecular basis for this effect.

At present, at least three different mechanisms are discussed for the action of amphipathic, lytic peptides. (i) The "carpet-like" mechanism (*15*, *16*) assumes the formation of a "peptide monolayer" that almost completely covers the surface of the vesicles. When a threshold concentration of bound peptide is reached, transient holes are formed resulting in vesicle lysis. (ii) The "class L" mechanism includes peptides with a narrow hydrophilic face containing Lys residues (*13*, *14*). These peptides are believed to destabilize biological membranes by the induction of negative curvature strain resulting in a localized disruption of the lipid bilayer structure. Magainin has been suggested to act by this mechanism (*13*, *39*). (iii) Pores have been proposed to be the mechanism of action of a multitude of lytic peptides and include a variety of pore structures (for review see refs 9 and 40). The group of Matsuzaki recently suggested a pore mechanism for the action of magainin 2 which includes the formation of a transient peptide−lipid supramolecular complex thus allowing not only the transport of ions but also the movement of peptide and lipid between the outer and inner monolayer (*10*).

Our investigations revealed that membrane permeabilization occurs when between 2 and 20 peptide molecules are bound per thousand lipid molecules. This number is much lower than necessary for the formation of a "peptide carpet". Therefore, a "carpet-like" mechanism is unlikely to be the mode of action of these peptides.

All angle-modified analogs raised the bilayer to hexagonal phase transition temperature of DPoPE (T_H) and hence reduced the intrinsic negative curvature strain of the bilayer. This is equivalent to the induction of positive curvature strain in flat, stable membranes, such as phosphatidylcholine. Thus, the class L mechanism recently suggested for magainin (*13*, *39*) can be excluded. Interestingly, differences between the analogs in the potential to increase T_H are mainly caused by differences in the binding. Again, analogs with an enhanced angle show a higher binding affinity than peptides with a smaller angle of positively charged residues. Therefore, all angle-modified analogs have, when lipid-bound, almost the same potential to induce positive curvature strain. This finding excludes pronounced differences in the membrane location of the peptides. As a consequence, all analogs are expected to be located parallel to the bilayer surface and close to the phospholipid headgroup region, as recently reported for magainin 2 (*36*, *41*).

The induction of positive curvature strain may also destabilize bilayers, possibly by the formation of micelles. Melittin has been shown to cause the micellization of phosphatidylcholine bilayers and to inhibit the formation of hexagonal phases of phosphatidylethanolamine (*12*, *42*). Therefore, it had to be clarified, whether the induction of positive curvature strain is the mechanism of bilayer permeabilization of the angle-modified peptides. To test this hypothesis dye-releasing experiments from (NMe)DOPE, a lipid with an intrinsic negative curvature strain, have been performed (Figure 8). The peptides with enhanced lipid affinities (140°M2a, 160°M2a, 180°M2a) increased a temperature-induced dye release at low peptide concentrations but inhibited it at higher peptide concentrations. The inhibition of temperature-induced dye release at higher

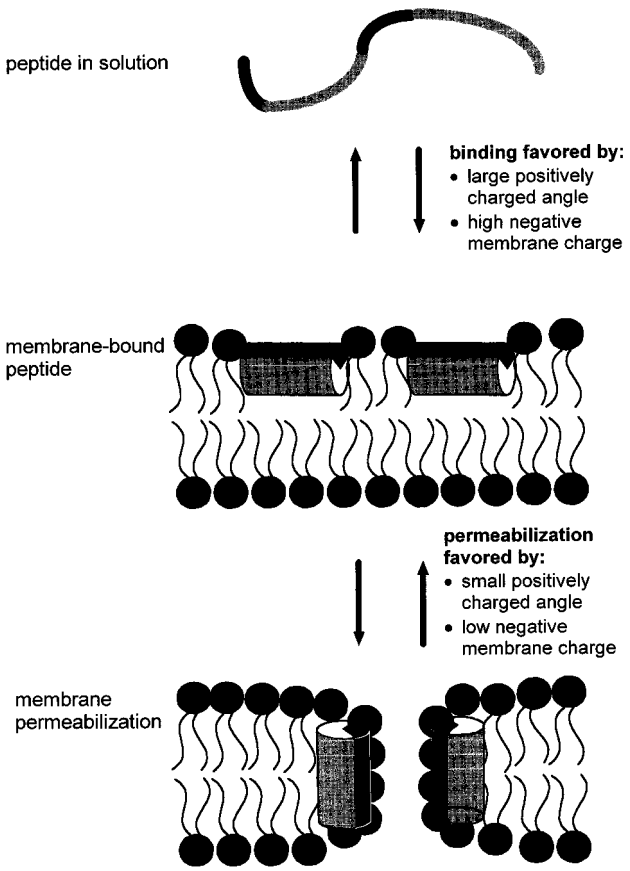

FIGURE 9: Cartoon illustrating the different effects of the angle circumscribed by the positively charged residues and the negative membrane charge on the binding and permeabilization stage of the peptide−membrane interaction: Binding is enhanced for analogs with a large angle of positively charged residues and on highly negatively charged membranes, whereas the membrane-permeabilizing efficiency of the bound peptide is favored by a small angle and a low negative membrane charge.

peptide concentrations can be explained by the membrane-stabilizing effect of the peptides due to the reduction of the existing negative curvature strain. The fact that a significant increase in membrane permeabilization occurs at lower peptide concentrations, under conditions of negative curvature strain, strongly indicates that the peptides do not permeabilize the membrane by induction of positive curvature strain. Therefore the action of the peptides on vesicles with an intrinsic negative curvature strain can be understood as an overlapping of two different effects: membrane destabilization by a permeabilization mechanism and membrane stabilization due to the reduction of negative curvature strain. The absence of the inhibition of dye release for analogs with small angles circumscribed by the positively charged residues seems rather to be a consequence of the reduced binding than of differences in the potential to reduce negative curvature strain (see Figure 7).

Our results are consistent with the pore mechanism recently suggested by Matsuzaki et al. (*10*) for the unmodified magainin 2. Analogs with a large angle subtended by the positively charged helix face can be expected to have an enhanced electrostatic repulsion among positively charged Lys residues of adjacent helices within the pore. In contrast, the repulsion should be minimized in analogs with a small angle of positively charged residues, where all Lys residues are directed into the pore interior. It is therefore reasonable to assume that the pore-forming probability and the pore life time decreases with increasing positively charged angle. This

corresponds well with our finding that the amount of bound peptide necessary for the induction of dye release increases with increasing angle (Figure 4B). Similar observations have recently been reported comparing magainin analogs with different positive overall charge (*43*). Despite better lipid binding, the dye releasing activity of an analog with increased positive charge was reduced. The authors explained the finding by an instability of the pore formed by this analog due to interhelical electrostatic repulsion.

CONCLUSIONS

Using a set of carefully designed magainin 2 amide analogs with differences in the angle subtended by the positively charged helix face, we showed that membrane-binding and permeabilizing efficiency are differently influenced by angle of the positively charged residues and by the membrane charge (Figure 9). Binding of the peptides to membranes is favored by a large angle and by a high negative membrane charge. In contrast, a small angle of positively charged residues and a low content of negatively charged phospholipids are of advantage for the membrane-permeabilizing efficiency of the bound peptide. The permeabilization of POPC-rich membranes as well as the biological activity are clearly dominated by the membrane affinity of the peptides. Our results are consistent with a pore mechanism for all analogs investigated.

ACKNOWLEDGMENT

We thank H. Nikolenko, A. Klose, D. Smettan, and B. Pisarz for excellent technical assistance.

REFERENCES

1. Habermann, E., and Jentsch, J. (1967) *Hoppe-Seyler's Z. Physiol. Chem. 348*, 37−50.
2. Hirai, Y., Yasuhara, T., Yoshida, H., Nakajiama, T., Fujino, M., and Kitada, C. (1979) *Chem. Pharm. Bull. Tokyo 27*, 1942−1944.
3. Ho, C.-L., and Hwang, L.-L. (1991) *Biochem. J. 274*, 453−456.
4. Hultmark, D., Steiner, H., Rasmuson, T., and Boman, H. G. (1980) *Eur. J. Biochem. 106*, 7−16.
5. Steiner, H., Hultmark, D., Engstrom, A., Bennich, H., and Boman, H. G. (1981) *Nature 292*, 246−248.
6. Lehrer, R. I., Ganz, T., and Selsted, M. E. (1991) *Cell 64*, 229−230.
7. Zasloff, M. (1987) *Proc. Natl. Acad. Sci. U.S.A. 84*, 5449−5453.
8. Maloy, W. L., and Kari, U. P. (1995) *Biopolymers 37*, 105−122.
9. Sansom, M. S. P. (1991) *Prog. Biophys. Mol. Biol. 55*, 139−235.
10. Matsuzaki, K., Murase, O., Fujii, N., and Miyajima, K. (1996) *Biochemistry 35*, 11361−11368.
11. Cruciani, R. A., Barker, J. L., Durell, S. R., Raghunathan, G., Guy, H. R., Zasloff, M., and Stanley, E. F. (1992) *Eur. J. Pharmacol. 226*, 287−296.
12. Batenburg, A. M., and DeKruijff, B. (1988) *Biosci. Rep. 8*, 299−307.
13. Tytler, E. M., Segrest, J. P., Epand, R. M., Nie, S. Q., Epand, R. F., Mishra, V. K., Venkatachalapathi, Y. V., and Anantharamaiah, G. M. (1993) *J. Biol. Chem. 268*, 22112−22118.
14. Epand, R. M., Shai, Y., Segrest, J. P., and Anantharamaiah, G. M. (1995) *Biopolymers 37*, 319−338.
15. Pouny, Y., Rapaport, D., Mor, A., Nicolas, P., and Shai, Y. (1992) *Biochemistry 31*, 12416−12423.
16. Gazit, E., Boman, A., Boman, H. G., and Shai, Y. (1995) *Biochemistry 34*, 11479−11488.
17. Merrifield, R. B., Merrifield, E. L., Juvvadi, P., Andreu, D., and Boman, H. G. (1994) in *Antimicrobial Peptides*, Ciba Foundation Symposium 186, pp 5−26, Wiley, Chichester, U.K.
18. Saberwal, G., and Nagaraj, R. (1994) *Biochim. Biophys. Acta 1197*, 109−131.
19. Dathe, M., Schümann, M., Wieprecht, T., Winkler, A., Beyermann, M., Krause, E., Matsuzaki, K., Murase, O., and Bienert, M. (1996) *Biochemistry 35*, 12612−12622.
20. Shai, Y., and Oren, Z. (1996) *J. Biol. Chem. 271*, 7305−7308.
21. Blondelle, S. E., and Houghten R. A. (1992) *Biochemistry 31*, 12688−12694.
22. Pathak, N., Salas-Auvert, R., Ruche, G., Janna, M. H., McCarthy, D., and Harrison, R. G. (1995) *Proteins: Struct., Funct., Genet. 22*, 182−186.
23. Dathe, M., Wieprecht, T., Nikolenko, H., Handel, L., Maloy, W. L., MacDonald, D. L., Beyermann, M., and Bienert, M. (1997) *FEBS Lett. 403*, 208−212.
24. Wieprecht, T., Dathe, M., Beyermann, M., Krause, E., Maloy, W. L., MacDonald, D. L., and Bienert, M. (1997) *Biochemistry 36*, 6124−6132.
25. Segrest, J. P., De Loof, H., Dohlman, J. G., Brouillette, C. G., and Anantharamaiah, G. M. (1990) *Proteins: Struct., Funct., Genet. 8*, 103−117.
26. Beyermann, M., Wenschuh, H., Henklein, P., and Bienert, M. (1992) in *Innovation and Perspectives in Solid Phase Synthesis* (Epton, R., Ed.) pp 349−353, Intercept Limited, Andover, U.K.
27. Hope, M. J., Bally, M. B., Webb, G., and Cullis, P. R. (1985) *Biochim. Biophys. Acta 812*, 55−65.
28. Böttcher, C. J. F., van Gent, C. M., and Pries, C. (1961) *Anal. Chim. Acta 24*, 203−204.
29. Chen, Y. H., Yang, J. T., and Martinez, H. M. (1972) *Biochemistry 11*, 4120−4131.
30. Lakowicz, J. R. (1983) in *Principles of Fluorescence Spectroscopy*, Plenum Press, New York.
31. Schwarz, G., Gerke, H., Rizzo, V., and Stankowski, S. (1987) *Biophys. J. 52*, 685−692.
32. Matsuzaki, K., Harada, M., Handa, T., Funakoshi, S., Fujii, N., Yajima, H., and Miyajima, K. (1989) *Biochim. Biophys. Acta 981*, 130−134.
33. Wieprecht, T., Dathe, M., Schümann, M., Krause, E., Beyermann, M., and Bienert, M. (1996) *Biochemistry 35*, 10844−10853.
34. Schümann, M., Dathe, M., Wieprecht, T., Beyermann, M., and Bienert, M. (1997) *Biochemistry 36*, 4345−4351.
35. Eisenberg, D. (1984) *Ann. Rev. Biochem. 53*, 595−623.
36. Bechinger, B., Zasloff, M., and Opella, S. J. (1993) *Protein Sci. 2*, 2077−2084.
37. Monette, M., and Lafleur, M. (1995) *Biophys. J. 68*, 187−195.
38. Park, N. G., Yamato, Y., Lee, S., and Sugihara, G. (1995) *Biopolymers 36*, 793−801.
39. Tytler, E. M., Anantharamaiah, G. M., Walker, D. E., Mishra, V. K., Palgunachari, M. N., and Segrest, J. P. (1995) *Biochemistry 34*, 4393−4401.
40. Lohner K., and Epand, R. M. (1997) *Adv. Biophys. Chem. 6*, 53−66.
41. Matsuzaki, K., Murase, O., Tokuda, H., Funakoshi, S., Fujii, N., and Miyajima, K. (1994) *Biochemistry 33*, 3342−3349.
42. Dufourcq, J., Faucon, J. F., Fourche, G., Dasseux, J. L., Le Maire, M., and Gulik-Krzywicki, T. (1986) *Biochim. Biophys. Acta. 859*, 33−48.
43. Matsuzaki, K., Nakamura, A., Murase, O., Sugishita, K., Fujii, N., and Miyajima, K. (1997) *Biochemistry 36*, 2104−2111.

BI971398N